

# Nernst effect of epitaxial $\text{Y}_{0.95}\text{Ca}_{0.05}\text{Ba}_2(\text{Cu}_{1-x}\text{Zn}_x)\text{O}_y$ and $\text{Y}_{0.9}\text{Ca}_{0.1}\text{Ba}_2\text{Cu}_3\text{O}_y$ films

---

Kokanović, Ivan; Cooper, J. R.; Matusiak, M.

Source / Izvornik: **Physical Review Letters**, 2009, 102

Journal article, Published version

Rad u časopisu, Objavljena verzija rada (izdavačev PDF)

<https://doi.org/10.1103/PhysRevLett.102.187002>

Permanent link / Trajna poveznica: <https://urn.nsk.hr/urn:nbn:hr:217:124024>

Rights / Prava: [In copyright](#) / [Zaštićeno autorskim pravom.](#)

Download date / Datum preuzimanja: **2024-05-02**



Repository / Repozitorij:

[Repository of the Faculty of Science - University of Zagreb](#)



# Nernst Effect Measurements of Epitaxial $\text{Y}_{0.95}\text{Ca}_{0.05}\text{Ba}_2(\text{Cu}_{1-x}\text{Zn}_x)_3\text{O}_y$ and $\text{Y}_{0.9}\text{Ca}_{0.1}\text{Ba}_2\text{Cu}_3\text{O}_y$ Superconducting Films

I. Kokanović,<sup>1,2,\*</sup> J. R. Cooper,<sup>1</sup> and M. Matusiak<sup>1</sup>

<sup>1</sup>*Cavendish Laboratory, University of Cambridge, Cambridge CB3 0HE, United Kingdom*

<sup>2</sup>*Department of Physics, Faculty of Science, University of Zagreb, P.O. Box 331, Zagreb, Croatia*

(Received 23 May 2008; published 4 May 2009)

We report Nernst effect data for crystalline films of  $\text{Y}_{0.95}\text{Ca}_{0.05}\text{Ba}_2(\text{Cu}_{1-x}\text{Zn}_x)_3\text{O}_y$  (with  $x = 0, 0.02$ , and  $0.04$ ) and  $\text{Y}_{0.9}\text{Ca}_{0.1}\text{Ba}_2\text{Cu}_3\text{O}_y$  grown by pulsed laser deposition. We show that our own results and published data for LSCO are consistent with the theory of Gaussian superconducting fluctuations. We also show that Zn doping increases the Nernst coefficient simply because it reduces the in-plane conductivity.

DOI: 10.1103/PhysRevLett.102.187002

PACS numbers: 74.25.Fy, 74.40.+k, 74.62.Dh, 74.72.Bk

In conventional type II superconductors, the motion of Abrikosov vortices induced by a thermal gradient ( $\nabla_x T$ ), perpendicular to the magnetic field  $B$ , gives rise to a transverse electric field  $E_y$  and hence a Nernst voltage, the Nernst coefficient  $\nu$  being defined by the relation,  $\nu = \frac{E_y}{\nabla_x T B}$ . In some influential papers, measurements of significant Nernst signals over a broad temperature range *well above* the superconducting transition temperature ( $T_c$ ) have been reported, initially for  $\text{La}_{2-x}\text{Sr}_x\text{CuO}_4$  (LSCO) [1,2] and later for several other cuprate crystals [3,4]. These results have been interpreted as evidence for the existence of vortexlike excitations above  $T_c$ , and for two separate temperature scales for phase and amplitude fluctuations of the superconducting order parameter. It was suggested that the pseudogap (PG) is actually caused by superconducting fluctuations, in contradiction to arguments based on heat capacity studies [5]. Claims that the PG stays finite for all superconducting compositions rather than going to zero [5] for slightly overdoped samples, have also been based on the Nernst data [1,3].

More recently, by introducing controlled amounts of disorder by electron irradiation [6], Zn [7] or Ni [8] doping, other authors have shown that the onset of a larger Nernst signal is not linked to  $T^*$ , the characteristic energy scale of the PG.

Nernst effect studies of the cuprates also inspired an extension of the theory of superconducting fluctuations [9] by Ussishkin *et al.* [2] who showed that for weak (Gaussian) fluctuations (GF), the off-diagonal term,  $\alpha_{xy}^s$ , of the Peltier tensor is given by

$$\alpha_{xy}^s = \frac{k_B e}{3h} \frac{\xi_{ab}^2}{l_B^2 s} \frac{1}{\sqrt{1 + (2\xi_c/s)^2}}; \quad (1)$$

here  $\xi_{ab}$  and  $\xi_c$  are the temperature-dependent coherence lengths parallel and perpendicular to the layers,  $s$  is the interlayer spacing,  $l_B = (\hbar/eB)^{1/2}$  is the magnetic length, and the anisotropy  $\gamma = \xi_{ab}/\xi_c$ . The fluctuation contribution to the Nernst coefficient is given by

$$\nu_s = \alpha_{xy}^s / [\sigma(T)B], \quad (2)$$

where  $\sigma(T)$  is the total electrical conductivity. Ussishkin *et al.* [2] found that Gaussian superconducting fluctuations account well for Nernst data of optimally doped and overdoped  $\text{La}_{2-x}\text{Sr}_x\text{CuO}_4$  crystals with  $x = 0.20$  and  $0.17$  but for an underdoped sample with  $x = 0.12$  they suggested that stronger non-Gaussian fluctuations give a larger Nernst signal and also reduce  $T_c$  from the mean field value [10]. Recently their GF theory [2] was verified over a wide temperature range by experiments on thin amorphous low-temperature superconductors [12], this is especially important in view of an alternative theoretical viewpoint reported recently [13].

Here we report measurements of the Nernst effect for the same Ca and Zn substituted  $\text{YBa}_2\text{Cu}_3\text{O}_y$  (YBCO) epitaxial films for which in-plane resistivity and magnetoresistivity  $\rho(B, T)$ , and Hall coefficient  $R_H$ , data were previously reported [14]. We show that our Nernst data above  $T_c$  are consistent with GF theory [2]. Although the Nernst signal is more clearly visible in our Zn-doped samples, we argue that this is primarily because of their smaller conductivity. In contrast to the suggestion of Refs. [6,7], for our samples there is no evidence for the Nernst signal being enhanced by another mechanism such as inhomogeneous superconductivity. We also show that GF can account for the general behavior of Nernst data of LSCO [1] over the whole doping range. Our new results and our GF analysis of LSCO data show that superconducting fluctuations are weak except very close to  $T_c$ . This tends to rule out both vortexlike excitations and scenarios where there are preformed local pairs (large amplitude correlations) well above  $T_c$ .

Values of the hole concentration  $p$  determined from the room-temperature thermopower,  $S(290 \text{ K})$  [15], are given in Table I together with  $T_c$  values and transition widths (FWHM,  $\Delta T_c$ , in  $d\rho/dT$ ). Small changes in  $p$  have occurred since the previous work and therefore quantities such as  $\rho(B, T)$  and  $R_H$  were measured again below 120 K. In the Nernst setup used here the  $10 \times 5 \times 1 \text{ mm}^3$   $\text{SrTiO}_3$  substrate was glued between copper and stainless steel posts each holding a heater and a small Cernox thermometer. A sketch of the patterned thin film is shown in the inset to Fig. 1(a). The temperature gradient

TABLE I. Summary of results.

Sample Ca, Zn	$T_c$ (K)	$\Delta T_c$ (K)	$p$ (holes/Cu)	$\xi_{ab}$ (nm)	$\gamma$
0.05	84.2	0.6	$0.136 \pm 0.002$	$1.6 \pm 0.2$	$6.2 \pm 0.5$
0.05, 0.02	65.1	1	$0.159 \pm 0.004$	$1.9 \pm 0.2$	$7.2 \pm 0.5$
0.05, 0.04	33.3	1.5	$0.164 \pm 0.004$	$2.6 \pm 0.2$	$5.1 \pm 0.5$
0.1	80.6	0.7	$0.198 \pm 0.004$	$3.4 \pm 0.2$	$7.5 \pm 0.5$

of 2 or 4 K/cm was applied along the longitudinal direction,  $B$  was applied along the  $c$  direction of the film (perpendicular to the surface of the substrate) and the Nernst signal was measured between the “Hall contacts” using a Keithley Model 182 nanovoltmeter. The transverse voltage  $V_B$  was measured for  $+B$  and  $-B$  while sweeping either  $T$  or  $B$ , the Nernst voltage was defined as  $\frac{1}{2}(V_B - V_{-B})$  and converted to electric field using the distance (1.5 mm) between the inside edges of opposite gold contact pads.  $\nabla T$  was checked by measuring the thermoelectric voltage between two longitudinal contacts. The precise temperature of the sample was determined by comparing  $\rho(T, B)$  data measured with and without an applied temperature gradient.

Zero-field  $\rho(T)$  data for the four films are shown in Fig. 1(a). Representative  $\rho(T, B)$  and Nernst data are shown for the over-doped 10% Ca sample ( $p = 0.198$ ) in Fig. 1(b) and for the most under-doped 5% Ca sample ( $p = 0.136$ ) in Fig. 1(c). The  $\rho(T, B)$  curves show the “fanning out” property typical of the cuprates that is not observed in conventional type II superconductors. The points at which  $\rho(T, B) \approx 0$  on the scales shown correspond to the irreversibility line  $B_{irr}(T)$ .

If one assumes that vortices are still present well above  $B_{irr}(T)$  [16] then the ratio  $\nu(T, B)/\rho(T, B)$  can be used to determine the entropy per vortex as has been done for LSCO [20]. This assumes isotropic vortex pinning forces, since the resistivity arises from sideways motion of the vortices (perpendicular to the direction of current flow) while the Nernst voltage arises from the flow of vortices along the length of the sample. In Fig. 1(b) the onset of the Nernst signal is the same as the onset of resistivity to within experimental uncertainty of  $\pm 0.5$  K. This was true for the three over- and optimally-doped samples studied. However data for the under-doped 5% Ca sample in Fig. 1(c) show sizeable Nernst signals  $\sim 6$  K below the points at which  $\rho(T, B) = 0$ . At the present time we do not know whether this unusual behavior is caused by the lower value of  $p$  (underdoping) or some other effect, for example, anisotropic vortex pinning. Vortex pinning at twin boundaries is known to be important in YBCO based compounds and can be highly anisotropic [21].

Figure 2 shows the Nernst coefficient above  $T_c$  for all four samples at  $B = 3$  or 6 T, vs the reduced temperature  $t \equiv (T - T_c)/T_c$  up to  $t = 0.6$ . As  $T_c$  is approached from above, field sweeps at fixed  $T$  become

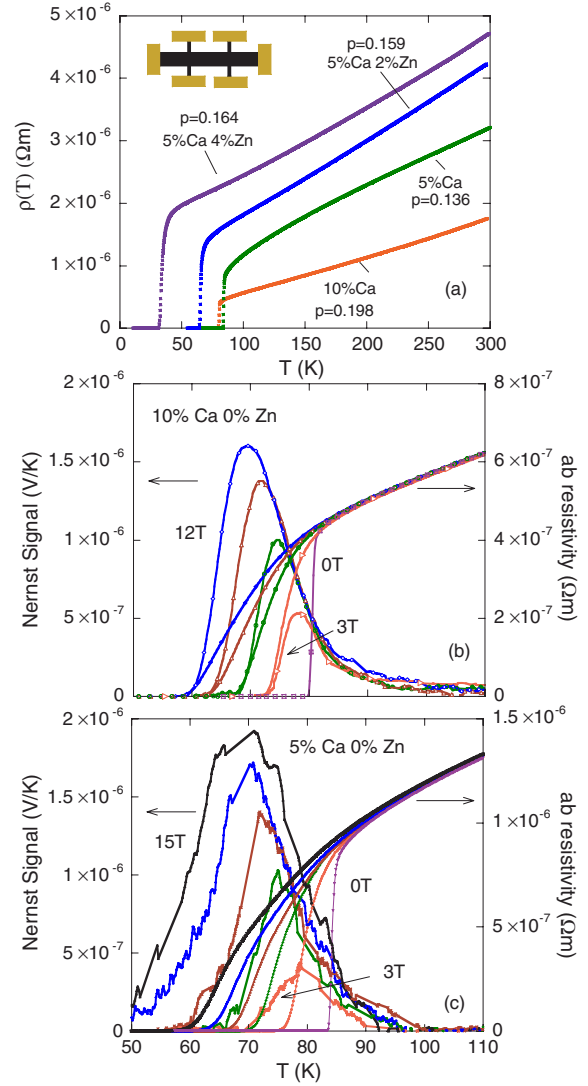


FIG. 1 (color online). (a) In-plane resistivity versus temperature for  $\text{Y}_{0.95}\text{Ca}_{0.05}\text{Ba}_2(\text{Cu}_{1-x}\text{Zn}_x)_3\text{O}_y$  ( $x = 0, 0.02$ , and  $0.04$ ) and  $\text{Y}_{0.9}\text{Ca}_{0.1}\text{Ba}_2\text{Cu}_3\text{O}_7$  films. (b) Nernst signal versus  $T$  at  $B = 3, 6, 9$  and  $12$  T for the  $\text{Y}_{0.9}\text{Ca}_{0.1}\text{Ba}_2\text{Cu}_3\text{O}_7$  film. (c) Nernst signal versus  $T$  at  $B = 3, 6, 9, 12$ , and  $15$  T for the  $\text{Y}_{0.95}\text{Ca}_{0.05}\text{Ba}_2\text{Cu}_3\text{O}_y$  film. In (b) and (c) in-plane resistivities at the same fields and at 0 T are also shown.

nonlinear at a field of  $1-2 \times (T - T_c)$  T. This is to be expected for GF which are gradually suppressed when  $l_B$  becomes comparable with  $\xi_{ab}(T)$ , or equivalently when  $B \sim (T - T_c) |dB_{c2}/dT|$ , where  $dB_{c2}/dT$  is the slope of  $B_{c2}$  just below  $T_c$  and is 1–2 T/K for cuprates with  $T_c$  values of 80 to 90 K.

The criterion used in Ref. [1] for a significant “vortex” signal is  $\nu = 4$  nV/K T. At first sight this might suggest that there are vortices up to  $t \approx 0.6$  in our 4% Zn-doped sample, and that disorder increases the temperature difference between the formation of fluctuating Cooper pairs and the onset of phase coherence, as proposed for electron-irradiated YBCO samples [6]. However, we question this

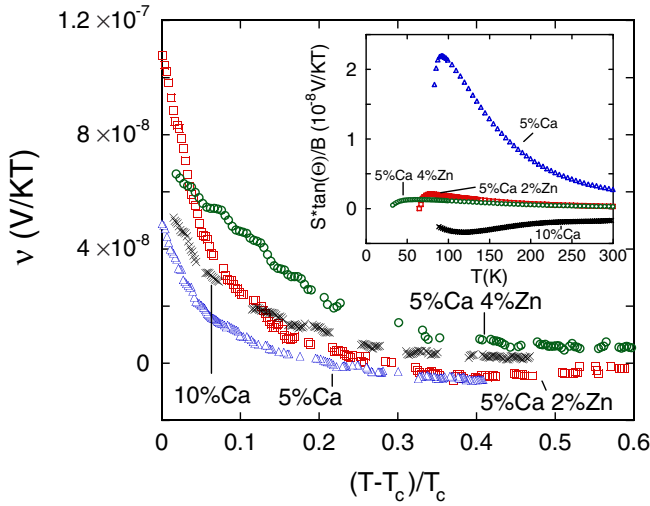


FIG. 2 (color online). Nernst coefficient,  $\nu$ , at  $B = 3$  T (6 T for 5% Ca 0 Zn) versus  $t$  for the  $Y_{1-x}Ca_xBa_2(Cu_{1-x}Zn_x)_3O_y$  ( $z = 0.05, 0.1$ ;  $x = 0, 0.02$ , and  $0.04$ ) films. Inset shows  $S \tan(\theta)/B$ , for the same samples, where  $S$  is the thermopower and  $\theta$  the Hall angle in a field  $B = 6$  T.

interpretation and argue below that the observed value of  $\nu$  arises simply from GF. The main reason for the enhancement of  $\nu$  by Zn doping is simply that it decreases  $\sigma_{xx}$ , [Eq. (2)] giving larger values of  $\nu$  for the same values of  $\alpha$ , which is turn is mainly dependent on the in-plane coherence length. Another reason is that Zn doping suppresses the normal state (quasiparticle) contribution  $\nu_n$ , since  $|\nu_n| \leq |S \tan \theta_H|$  where  $S$  is the thermoelectric power and  $\theta_H$  the Hall angle [22]. As shown in the inset to Fig. 2, for the two Zn-doped films,  $S \tan \theta_H$  is particularly small and this makes the GF term even more visible.

Figure 3 shows  $\alpha/B \equiv \sigma_{ab}(T)\nu$  vs  $t$  for the data in Fig. 2 and fits to Eq. (1) in the linear region  $E_y \propto B$ , with  $s = 1.17$  nm, the  $c$ -axis lattice parameter. An extra fitting parameter, a small offset  $\approx -0.01$  V/K T  $\Omega$  m, has been included in Eq. (1) to account for  $\nu_n$ . In the 3D limit of Eq. (1) near  $T_c$  where  $\xi_c(T) \gg s$ , we expect  $\alpha^{-2} \propto (T - T_c)$ . Corresponding plots are shown in the inset to Fig. 3. There are small linear regions 2–3 K wide, extrapolating to  $y = 0$  near the measured value of  $T_c$ . At higher  $T$  these cross over to the quadratic law,  $\alpha^{-2} \propto (T - T_c)^2$  expected in the 2D limit. A similar analysis [23] of the heat capacity of several cuprate families showed that the difference,  $\delta T_c$ , between the measured value,  $T_c^m$ , and the fitted or linearly extrapolated value,  $T_c^f$ , was caused by strong (critical) fluctuations.  $\delta T_c$  was  $\sim 1$  K for YBCO samples, as found for the present Nernst data, and  $\sim 5$  K for other extremely anisotropic cuprates.

The fitting parameters  $\xi_{ab}(T = 0)$  and  $\gamma \equiv \xi_{ab}/\xi_c$  are summarized in Table I. The value  $\xi_{ab}(0) = 1.6$  nm for the 5% Ca sample corresponds to  $B_{c2}(0) \equiv \Phi_0/2\pi\xi_{ab}(0)^2 = 130$  T for  $B \parallel c$  and also agrees with the value obtained by GF analysis of heat capacity data [23]. The value of  $\gamma$  also

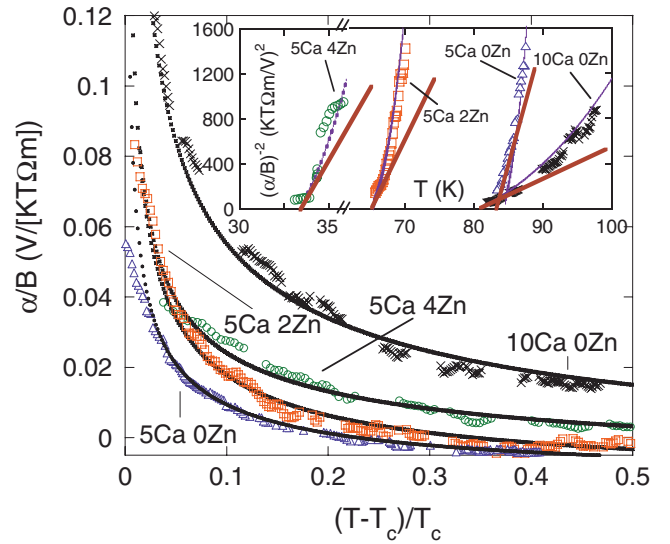


FIG. 3 (color online).  $\alpha/B \equiv \sigma_{ab}(T)\nu$  vs  $(T - T_c)/T_c$  for  $Y_{0.95}Ca_{0.05}Ba_2(Cu_{1-x}Zn_x)_3O_y$  ( $x = 0, 0.02, 0.04$ ) and  $Y_{0.9}Ca_{0.1}Ba_2Cu_3O_y$  films. Dotted lines show fits to Eq. (1). Data taken at 3 T are shown except for 5% Ca 0 Zn, where 6 T data are fitted down to  $T_c + 3$  K. The insets are plots of  $(\alpha/B)^{-2}$  at 3 T vs  $T$  near  $T_c$ , with dashed or lighter lines showing the fits to Eq. (1) and heavy lines the linear 3D limit of Eq. (1).

agrees with other estimates for YBCO<sub>y</sub> with  $y = 6.7$  to  $6.9$  [17]. GF analysis of  $\nu(T)$  data for a second under-doped sample [24] with  $T_c = 81.7$  K and  $p = 0.12$  gave a similar value,  $\xi_{ab}(0) = 1.4(6)$  nm. The values of  $\xi_{ab}(0)$  for the two Zn-doped films are larger. For the 2% Zn film,  $1/\xi_{ab}(0)$  scales with  $T_c$  as expected, but for the 4% Zn film the short mean free path probably reduces  $\xi_{ab}(0)$  according to the standard dirty-limit formula [25]. The coherence length of the 10% Ca, 0% Zn film is longer than that for the 5% Ca, 0% Zn film. This is not understood; however,  $\rho(T)$  is a factor of 2 smaller, and also for 10% Ca, Eq. (1) gives a good fit with  $\xi_{ab}(0) = 2.2$  nm and  $\gamma = 12$  over a smaller range of  $t$  (between 0.03 and 0.2).

The success of the GF analysis described above encouraged us to look again at published data for LSCO crystals, since Fig. 4 of Ref. [1] and other versions [3,22] provide key support for the alternative, widely accepted, phase fluctuation and pseudogap pictures. In Fig. 4(a) we show values of  $\gamma$  obtained from the anisotropy in the London penetration depth at low  $T$  [26,27] and from that in  $\rho(300$  K) [28] as well as values of  $\xi_{ab}(0)$  obtained from GF analysis [23] of the electronic specific heat [5] above  $T_c$ . These have been used in Eqs. (1) and (2), together with the measured values of  $T_c(x)$  [5] and  $\rho_{ab}(T, x)$  [11,28], to calculate the contour plots for  $\nu$  shown in Fig. 4(b). This GF picture correctly accounts for the peaked structure of  $\nu$  vs Sr content ( $x$ ) and the magnitude of  $\nu$  between 40 and 80 K [1,3,22]. The asymmetric GF peak arises from the dome-shaped  $T_c(x)$  curve and the approximately linear increase of  $\sigma_{ab}(T)$  with  $x$  [11,28]. Above 80 K GF theory



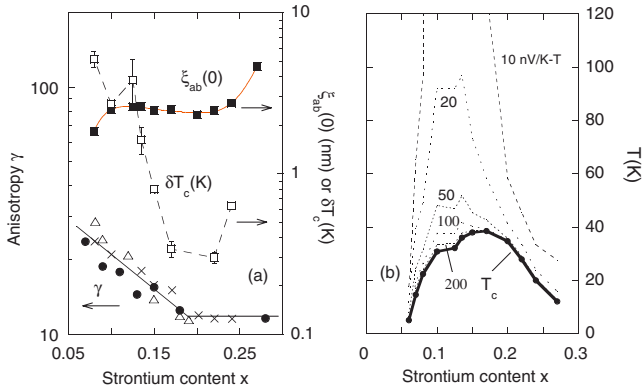


FIG. 4 (color online). (a) Left-hand scale, anisotropy,  $\gamma \equiv \xi_{ab}(0)/\xi_c(0)$ , obtained from the room-temperature resistivity anisotropy [28] (●) and two sets of London penetration depth data at low  $T$  (×) [26] and (△) [27], vs Sr content  $x$  in LSCO. Straight lines show average values of  $\gamma$  used in calculations. Right-hand scale,  $\xi_{ab}(0)$  obtained from a GF analysis [23,29] of heat capacity ( $C_v$ ) data [5] above  $T_c$  using the same values of  $\gamma$ .  $\delta T_c(x)$  [29] is related to the strength of critical (non-Gaussian) fluctuations [23]. (b) Calculated constant  $\nu$  contours in the  $(T, x)$  plane, using Eqs. (1) and (2), with  $s = 0.66$  nm,  $\rho_{ab}(x, T)$  from Ref. [11] and  $\xi_{ab}(0)$  and  $\gamma$  from Fig. 4(a).

gives values of  $\nu$  which are too large, possibly because the fluctuations are suppressed by inelastic scattering processes. In the experimental contour plot [1] there is a small region,  $x \leq 0.13$  and  $T - T_c \leq 5$  K, where  $\nu \approx 500$  nV/K T is too large to be consistent with GF theory. Figure 4(a) shows that  $\delta T_c \sim 2$ –5 K for  $x \leq 0.13$ , supporting the idea [2] that in this small region [10]  $\nu$  is enhanced by critical (non-Gaussian) fluctuations.

In summary we find that weak (Gaussian) superconducting fluctuations account for our Nernst data for YBCO  $ab$ -plane films substituted with various levels of Ca and Zn, until at least 30 K above  $T_c$ . They also account for the main features of the Nernst contour plots for LSCO crystals from  $x = 0.06$  to 0.27.

We are grateful to J.W. Loram and S.H. Naqib for fruitful collaboration and many useful suggestions. This work was supported by EPSRC (UK), Grant No. EP/C511778/1 and the Croatian Research Council, MZOS Project No. 119-1191458-1008.

\*kivan@phy.hr

- [1] Z. A. Xu, N. P. Ong, Y. Wang, T. Kakeshita, and S. Uchida, *Nature* (London) **406**, 486 (2000).
- [2] I. Ussishkin, S. L. Sondhi, and D. A. Huse, *Phys. Rev. Lett.* **89**, 287001 (2002).
- [3] Y. Wang, L. Li, and N. P. Ong, *Phys. Rev. B* **73**, 024510 (2006).
- [4] Pengcheng Li, Soumen Mandal, R. C. Budhani, and R. L. Greene, *Phys. Rev. B* **75**, 184509 (2007).
- [5] J. W. Loram, J. Luo, J. R. Cooper, W. Y. Liang, and J. L. Tallon, *J. Phys. Chem. Solids* **62**, 59 (2001).
- [6] F. Rullier-Albenque, R. Tourbot, H. Alloul, P. Lejay, D. Colson, and A. Forget, *Phys. Rev. Lett.* **96**, 067002 (2006).
- [7] Z. A. Xu, J. Q. Shen, S. R. Zhao, Y. J. Zhang, and C. K. Ong, *Phys. Rev. B* **72**, 144527 (2005).
- [8] N. Johansson, Th. Wolf, A. V. Sologubenko, T. Lorenz, A. Freimuth, and J. A. Mydosh, *Phys. Rev. B* **76**, 020512 (R) (2007).
- [9] A. Larkin and A. Varlamov, *Theory of Fluctuations in Superconductors* (Clarendon Press, Oxford (U.K.), 2005).
- [10] Using Nernst [3] and resistivity [11] data for LSCO with  $x = 0.12$  we find  $\alpha$  values that are a factor of 2 less than those given in Fig. 1 of Ref. [2]. As a result there are only significant deviations from the GF formula, Eq. (2) at 40 K and below.
- [11] Y. Ando, S. Komiya, K. Segawa, S. Ono, and Y. Kurita, *Phys. Rev. Lett.* **93**, 267001 (2004).
- [12] A. Pourret *et al.*, *Nature Phys.* **2**, 683 (2006).
- [13] A. Sergeev, M. Y. Reizer, and V. Mitin, arXiv0708.1003v1 [*Phys. Rev. B* (to be published)].
- [14] I. Kokanović, J. R. Cooper, S. H. Naqib, R. S. Islam, and R. A. Chakalov, *Phys. Rev. B* **73**, 184509 (2006).
- [15] S. D. Obertelli, J. R. Cooper, and J. L. Tallon, *Phys. Rev. B* **46**, 14 928 (1992).
- [16] For  $B > B_{ir}(T)$  the accepted picture is that of a “vortex liquid”, but thermodynamic fluctuations are also important here [17,18], in agreement with a recent dynamical scaling analysis of voltage-current measurements for YBCO single crystals and films [19].
- [17] D. Babić, J. R. Cooper, J. W. Hodby, and C. Changkang, *Phys. Rev. B* **60**, 698 (1999).
- [18] J. R. Cooper, J. W. Loram, J. D. Johnson, J. W. Hodby, and C. Changkang, *Phys. Rev. Lett.* **79**, 1730 (1997).
- [19] S. Li *et al.*, arXiv:0803.0969v1.
- [20] C. Capan *et al.*, *Phys. Rev. Lett.* **88**, 056601 (2002).
- [21] S. Fleshler *et al.*, *Phys. Rev. B* **47**, 14448 (1993).
- [22] Y. Wang *et al.*, *Phys. Rev. B* **64**, 224519 (2001).
- [23] J. W. Loram, J. R. Cooper, J. M. Wheatley, K. A. Mirza, and R. S. Liu, *Philos. Mag.* **65**, 1405 (1992).
- [24] M. Matusiak, S. H. Naqib, I. Kokanović, and J. R. Cooper, *Europhys. Lett.* **86**, 17 005 (2009).
- [25] J. R. Waldram, *Superconductivity of Metals and Cuprates* (IOP, Bristol, 1996), Chap. 10.
- [26] C. Panagopoulos, T. Xiang, W. Anukool, J. R. Cooper, Y. S. Wang, and C. W. Chu, *Phys. Rev. B* **67**, 220502(R) (2003).
- [27] T. Shibauchi, H. Kitano, K. Uchinokura, A. Maeda, T. Kimura, and K. Kishio, *Phys. Rev. Lett.* **72**, 2263 (1994).
- [28] T. Kimura *et al.*, *Phys. Rev. B* **53**, 8733 (1996).
- [29] Data for the electronic heat capacity,  $C_v$ , of LSCO [5] were fitted to the GF expression [Eq. (1) of Ref. [23]] plus a linear background. Here  $\delta T_c \equiv T_c^m - T_c^f$ , where  $T_c^m$  is the midpoint of the step in  $C_v/T$  and  $T_c^f$  is obtained from the GF fits.